S-AA-M-31

Cryogenic Target Handling System Operations Manual Volume IV–CTHS Description

Chapter 8: Characterization Station (CS)

Table of Contents

Chapter 8
Characterization Station (CS)

8.1 INTRODUCTION

To achieve high gain and ignition in inertial confinement fusion (ICF) implosions, the targets must be driven by a very uniform laser pulse and the plasma must remain symmetrical during the resulting radial compression until high temperatures and densities are created. The Rayleigh–Taylor (RT) instability is a fluid flow phenomenon that causes an initially uniform flow to disintegrate into turbulence. In ICF, the RT effect tends to limit compression densities by destroying the symmetry of the implosion. Because target imperfections can seed RT, the ice layer in cryogenic targets must be very uniform. The thickness and uniformity of the ice are critical parameters in the assessment of the results of target shots.

Shadowgraphic images of the targets for shots 24089 and 24096 are shown in comparison with static x-ray pinhole camera (XRPC) images and x-ray framing camera (XRFC) snapshots (Fig. 8.1-1). The XRPC images show the lighting up of the thin plastic shell on the outside of the target and the formation of a core in the center of the image. The XRFC images are recorded at peak compression with an exposure time of 40 ps. A clear correlation of the layer quality in the shadowgraphic images and the core quality in the XRPC and XRFC images can be seen.

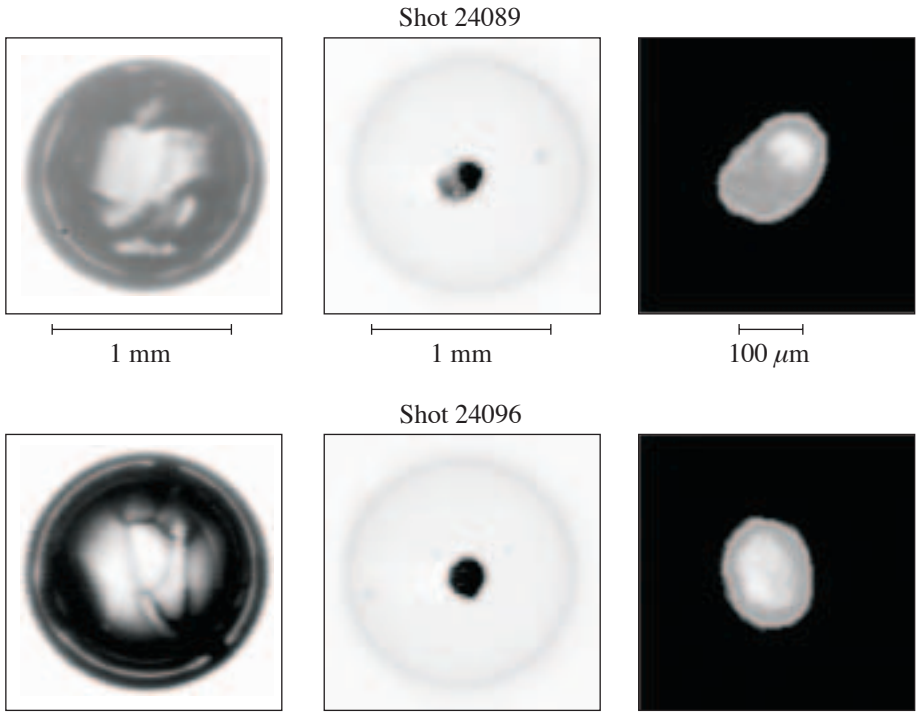

Figure 8.1-1
Ice-layer quality has a direct impact on the core quality.

Two identical characterization stations, one of which is shown in Fig. 8.1-2, are located in Room 157. They are used to image the contents of targets in order to diagnose the state of the fuel and to characterize the ice layers formed during the laying process. Each characterization station (CS) consists of an optical table that is fitted with a moving cryostat docking station and a two-axis viewing system, which includes a science-grade CCD camera. The optical table is mounted on an active vibration isolation system and supported at an elevation that allows a moving cryostat transfer cart (MCTC) to be positioned under it. The moving cryostat (MC) can then be elevated into the docking station so that the target is visible to the viewing system.

The process that produces a layered target consists of three steps: (1) determination of the equipment settings that will cause the fuel to be at its triple-point temperature, (2) crystal formation and layering, and (3) characterization. The equipment in the MCTC is used to control the target environment and to position the target for viewing. The CS is used to acquire and analyze images. A comprehensive suite of software modules is used to facilitate the process. The software includes image analysis routines that produce ice-thickness and roughness values and can provide three-dimensional images for assessments.

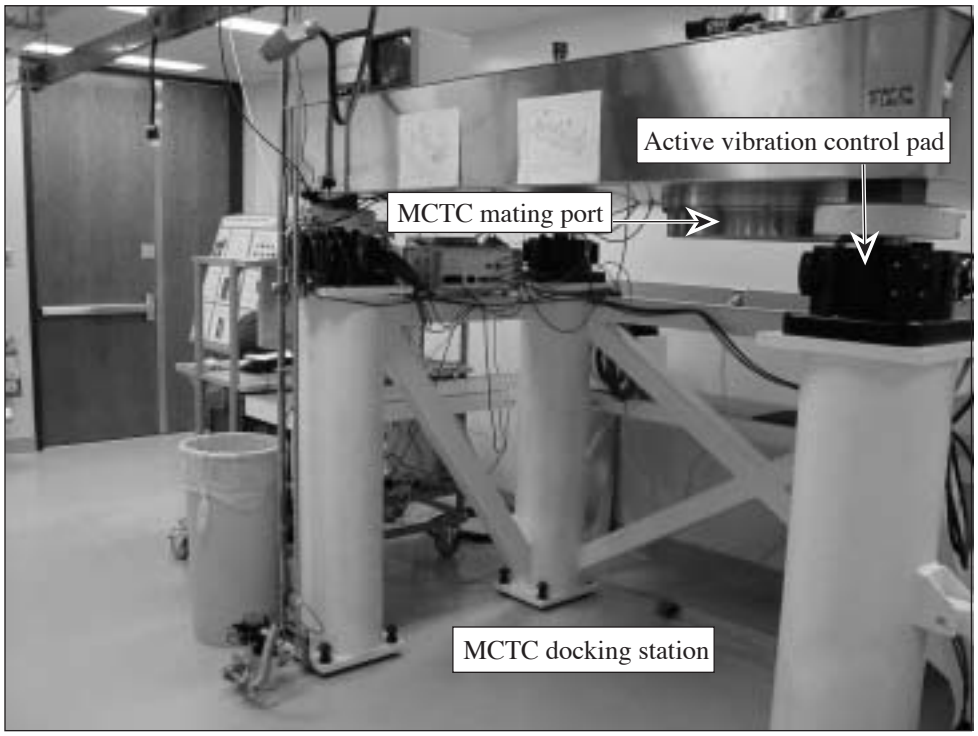

G6160

Figure 8.1-2
Characterization station showing the four pylons, MCTC docking station and mating port, and active vibration control pads.

8.2 EQUIPMENT DESCRIPTION

The relevant parts of the MCTC, the CS, and the controls and software are discussed in this section. Figure 8.2-1 shows these items and their relationships.

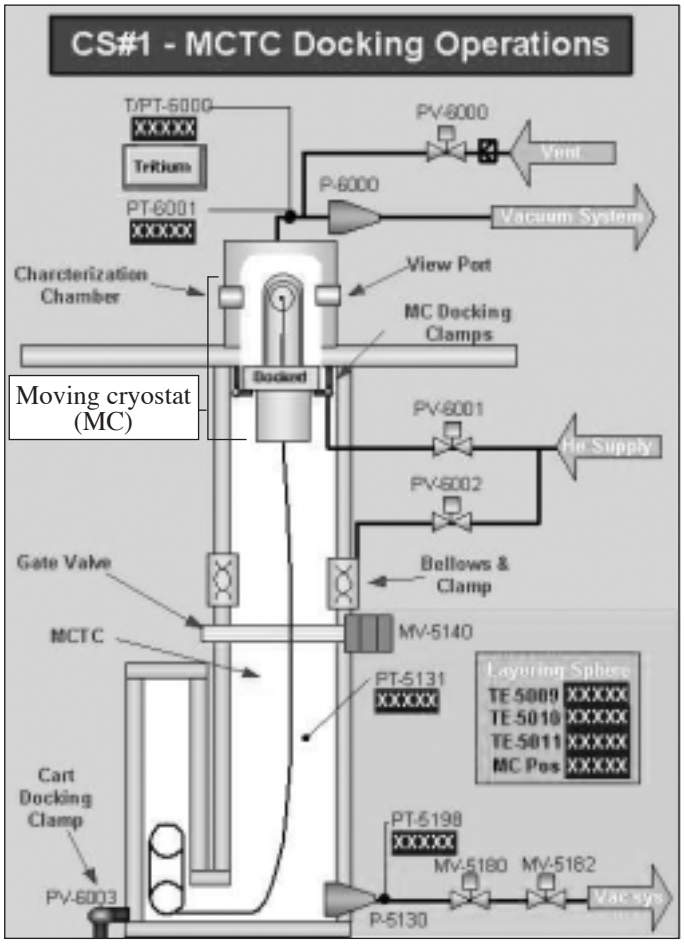

G6161

Figure 8.2-1
The characterization station and MCTC process diagram.

8.2.1 MCTC Items

The MCTC consists of the cooling, vacuum, and control equipment needed to support the target, transport it to various locations, and position it for viewing or shots. The MCTC turbo pump keeps the interior of the MCTC at high vacuum and exhausts to the Room 157 vacuum manifold system. The MCTC short-lift elevator raises the MC into the CS docking station. The MC includes the cold head, which creates and maintains the target's cryogenic temperature environment. It also includes the upper and lower shrouds, which insulate the target from the room-temperature vacuum housings, and the fine-motion stage, which supports and positions the target.

The MCTC also includes an optical parametric oscillator (OPO) laser and a precision resistance heater/controller that are used in the layering process.

8.2.1.1 Layering Sphere

At the upper end of the upper shroud is the gold-plated copper layering sphere that surrounds the target and is conductively connected to the cold head at the base of the MC.

Some of the features of the layering sphere are illustrated in Fig. 8.2-2 and include two of the four optical ports that are used to illuminate and view the target, the opening that clears the target and its support when the upper shroud is placed on the MC or removed from it, and the optical fiber that introduces IR energy from an external laser as part of the layering process.

The layering sphere is also equipped with a resistance heater and a temperature sensor. The interior surface of the layering sphere is roughened to enhance its thermal radiation characteristics so that it can function as an integrating sphere to bathe the target uniformly with thermal radiation from the fiber and its own emissions. (The data presented in Fig. 8.2-2 indicate that the "keyhole" and the viewing ports compromise this goal and produce ice-surface deviations that correlate with the openings in the sphere.)

Helium is introduced into the base of the MC and flows along the target support and into the layering sphere, where it acts as a conductive and convective heat exchange medium to enhance the thermal link between the target and the sphere.

The heat provided by the laser and the resistance heater is balanced against the cooling provided by the cold head to control the temperature of the layering sphere (and therefore the target) with ±1-mK precision.

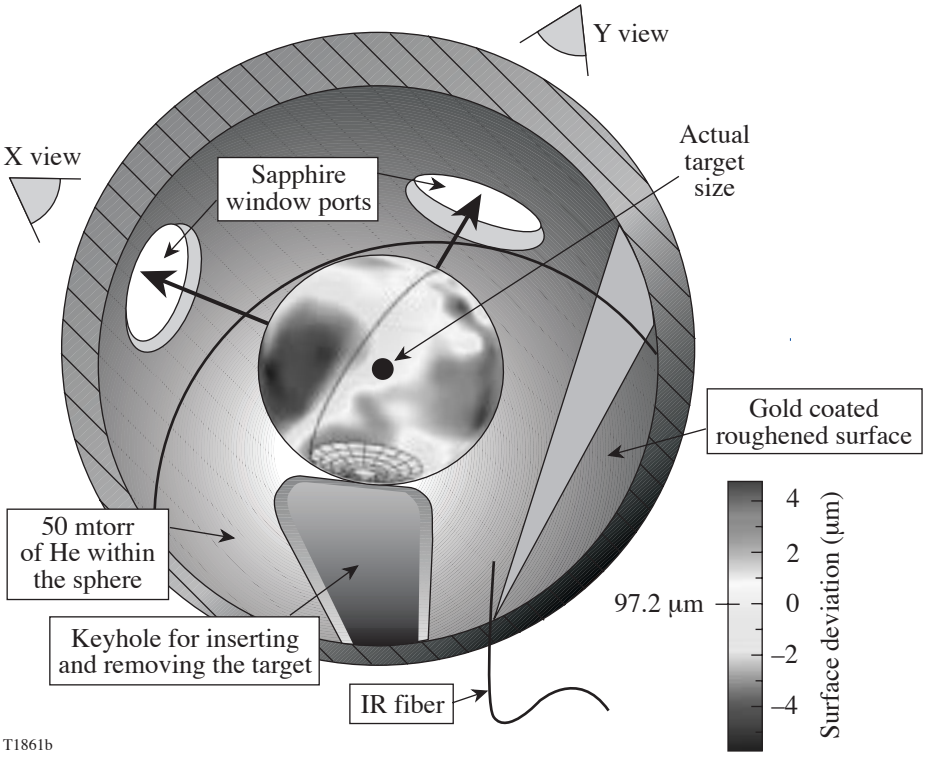

Figure 8.2-2
The MCTC layering sphere.

8.2.1.2 Optical Parametric Oscillator (OPO) Laser

The laser used to effect layering in the MC is an Acculight Model 1100 IR Laser with adjustable wavelength capability (described in more detail in the MCTC chapter). The laser is mounted on the MCTC and a single, 60-ft, slender fiber-optic cable transports the OPO IR power from the laser head to the layering sphere. The wavelength of the laser is set at 3.16 μm, which corresponds to an absorption peak for deuterium ice. Approximately 20% to 40% of the IR power is coupled into the layering sphere: the target absorbs a net 0.02% of the indicated OPO output power. Changing the laser output power by 0.1 mW changes the temperature of the target by 3 mK.

8.2.1.3 Layering Sphere Heater and Lakeshore Controller

A Lakeshore temperature controller controls the layering sphere temperature. The controller monitors the temperature via two redundant Cernox temperature sensors and adjusts the power to the two sets of heating tape (10 watt), which are wrapped on the outside of the layering sphere.

8.2.2 Characterization Station Components

The key components of each CS are discussed in the following sections.

8.2.2.1 MCTC Docking Station

The provisions for docking MCTC's are illustrated in Fig. 8.2-1. A characterization chamber vacuum vessel houses the MC when it is extended upward from the MCTC. The upper portion of this chamber extends above the optical table and includes viewing ports that are aligned with the ports in the upper shroud. The lower portion of this chamber includes the docking plate and clamps that mate with the MC. A 16-in. flexible bellows and clamp assembly provides the vacuum connection to the MCTC. The characterization chamber is connected to the Room 157 vacuum manifold system.

A pneumatically actuated cart-docking clamp anchors the MCTC to the floor after it has been correctly positioned under the CS.

8.2.2.2 Vibration Control System

The CS optical table is isolated from room vibrations by a STACIS 2000 Active Vibration Control System (supplied by Technical Manufacturing Corporation, Peabody, MA). This system provides wide-band vibration isolation (0.6 to 250 Hz). The vibration system isolates minute vibrations such as those from passing technicians, air handling systems, and the cart compressor (Fig. 8.2-3).

The STACIS 2000 system combines active vibration control based on piezoelectric actuators with passive isolation technology. The main components of the system are a user interface controller and four independent isolators positioned between the characterization station platform and the four support pillars. Each isolator houses five piezoelectric actuators and a passive rubber mount 100 times stiffer than standard pneumatic isolators.

The actuators control vibration along all three axes. The piezoelectric actuators receive information on disturbances through absolute velocity sensors. This information is used to command the actuators to expand or contract as required, attenuating vibration and diminishing its impact.

Figure 8.2-3
The components for the STACIS 2000 active vibration control system.

8.2.2.3 Camera Viewing System

Each CS is equipped with a camera viewing system as illustrated in Fig. 8.2-4. The system is used for target viewing and digital acquisition of images for analysis.

Illumination is provided by a computer-controlled, pulsed LED that is a fiber-coupled to collimation and focusing optics. The illumination is introduced through one of the viewing ports. The CCD camera views the backlighted target through the opposite viewing port. It is equipped with a 10× zoom lens, and the signal from the camera is connected to a frame grabber in the computer.

Dalsa Camera

The Dalsa 1M30 digital camera provides low-noise, high-sensitivity, 12-bit images with 1-k × 1-k spatial resolution at up to 30 frames per second (fps). The 1M30 is a frame transfer CCD camera that uses a progressive scan CCD to simultaneously achieve outstanding resolution and gray-scale characteristics (Fig. 8.2-5).

A square pixel format and high fill factor provide superior, quantifiable image quality even at low light levels. True 12-bit performance provides up to 4096 distinct gray levels and up to 8 × 8 binning.

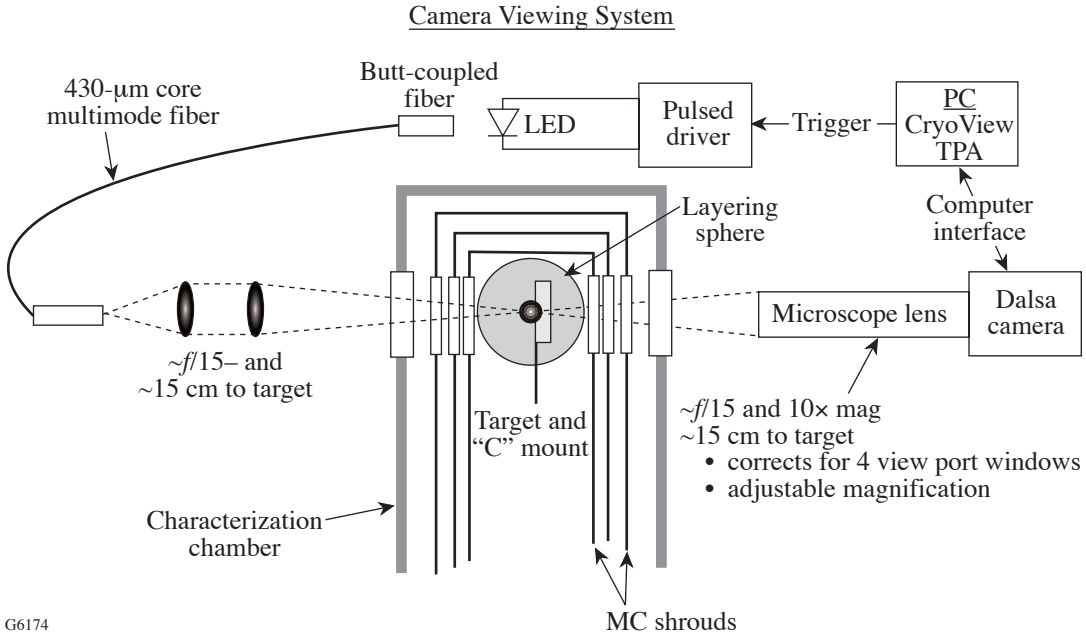

Figure 8.2-4
The characterization station camera viewing system.

Figure 8.2-5
The Dalsa camera.

Thales Optem Zoom Lens

This is an *f*/5 optic system with a 15-cm focal length that provides correction for the four optical windows that are between the zoom lens and the target. The lens package also has adjustable magnification and focus capabilities (Fig. 8.2-6).

The magnification of the optical system is calibrated using an accurately measured sapphire reference sphere. Currently, one pixel in the Dalsa camera equates to 1.09 μm and it can be used to measure the thickness of the ice layer to within 3%. If the optical system is moved, this calibration is voided and the magnification must be redetermined.

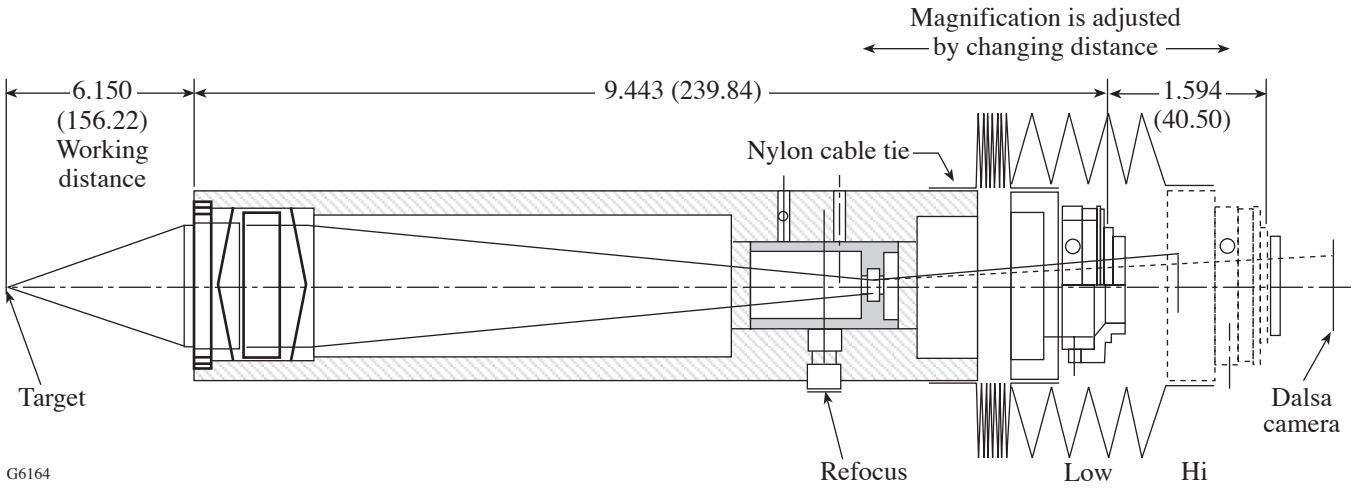

Figure 8.2-6
The Thales Optem Zoom Lens.

8.2.2.4 Characterization Station Server Software

A comprehensive suite of software modules supports CS operations. Figure 8.2-7 illustrates the overall architecture, which consists of a CS server that runs on the local PC, a CryoView client, an image analysis program that may be remote, interfaces to the CS and MCTC equipment, and database connections.

CryoView/Server

The CryoView software provides the operator interface to the Dalsa camera and the LED pulse driver. The software allows the operator to view and save images of the target. This operation acquires an image and saves it to a specified location as an HDF file. The operator is given an opportunity to accept or reject each image. The images acquired may be binned (2 × 2, 4 × 4, or 8 × 8). CryoView also provides the operator interface for the other functions provided by the CS server including image process data storage.

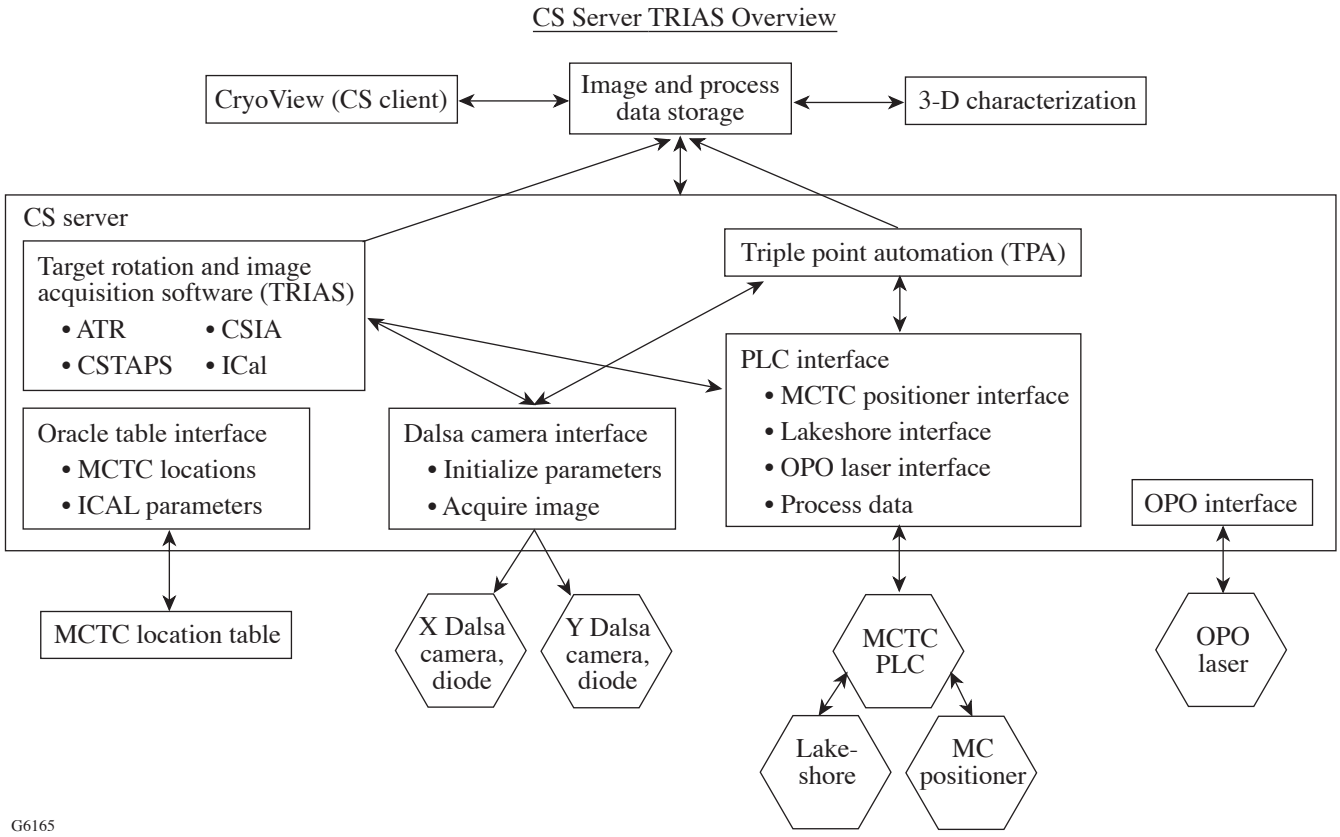

Figure 8.2-7
The cryo server functional overview diagram.

The CS server incorporates the communication and control interfaces to all of the external devices and systems that are needed to carry out target operations at the CS. In addition to those for the CCD camera and the LED illuminator, these include connecting to the PLC that controls the docked MCTC and the separate PC computer on the MCTC that controls the OPO laser. These and the connections to the LLE experimental database are implemented via Ethernet. Because the computers on the MCTC's have the same IP address wherever they are located in the facility, the CS server must access the database to get the addresses that apply to the MCTC that is currently at the CS.

The data exchanged between the server and the MCTC PLC include target-positioning commands, resistance heater set points for use by the Lakeshore controller, and the layering-sphere temperature data. The link with the OPO laser controller will include operating commands, layering-sphere temperature, and laser performance parameters.

The server includes two automated processes designed to reduce operator workload. Triple-point automation (TPA) steps the layering sphere through a range of temperatures and acquires a target image at steady-state conditions at each level. Subsequent manual analysis of the images allows determination of the equipment settings that will cause the fuel to be at its triple-point temperature (this process is discussed further in Sec. 8.3 below). The Target Rotation and Image Acquisition Software (TRIAS) will rotate the target on its axis to a series of stations. At each location, the target is automatically

centered in the camera's field of view, and an image of the ice layers is taken and stored for analysis. This image set provides the data needed to characterize the thickness and surface finish of the ice.

The main operator interface GUI is shown in Fig. 8.2-8). The horizontal and vertical light intensity bars are shown next to the acquired image. The operator can access the camera parameters, the Lakeshore temperature, and the TPA and TRIAS modules from the pulldown menus.

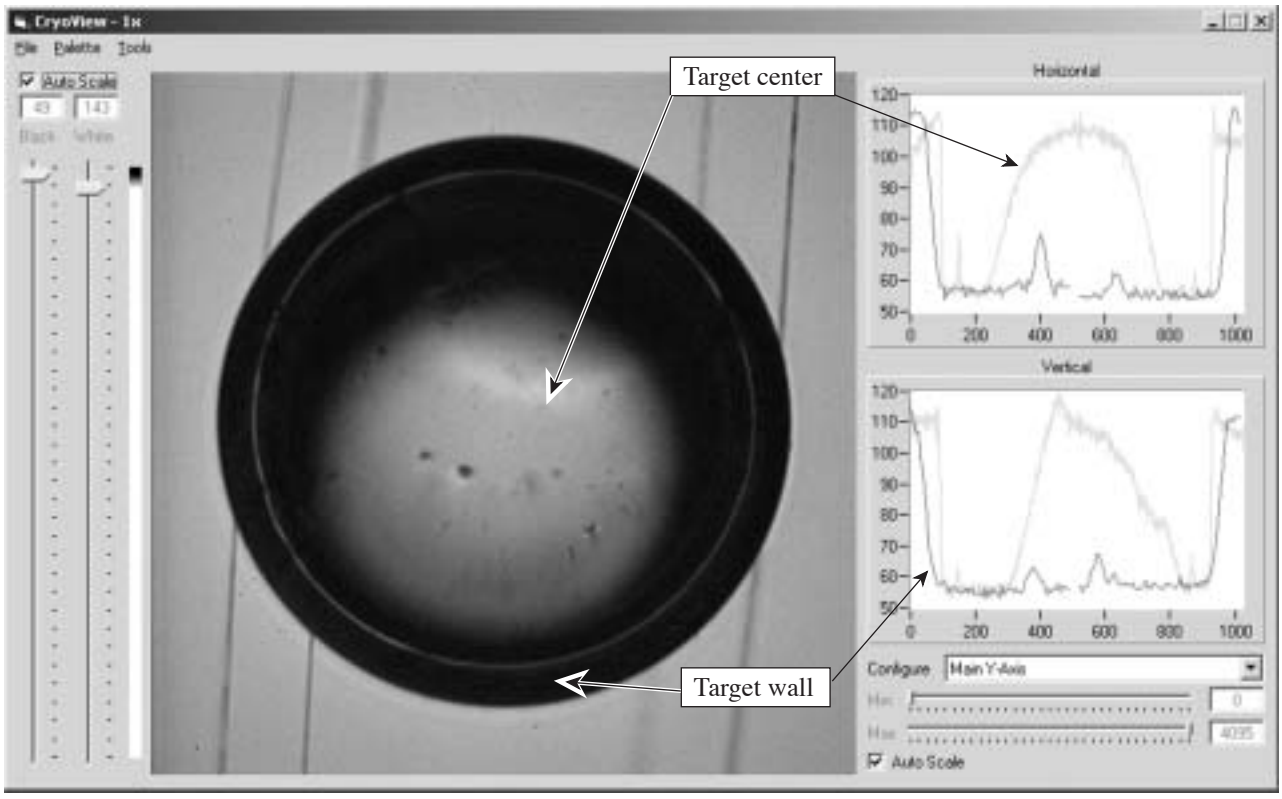

Figure 8.2-8
The CryoView display.

8.3 THE LAYERING PROCESS

The layering and characterization process can be divided into three steps:

(a) Layering
- Triple Point Temperature – Adjust target temperature to just below the triple point. This can be achieved by adjusting the OPO IR power setting or layering sphere temperature setpoint. The exchange gas pressure also impacts the response of the thermal exchange.
- Crystal formation phase – Crystal front growth advances by keeping target temperature just below the triple point (1 to 16 h).

(b) Characterization
- Characterization – Acquire and analyze images for multiple target rotations.

8.3.1 Layering Process Description

Forming an ice layer involves beginning with deuterium or tritium in the liquid/vapor phases and dropping the temperature on the layering sphere to initiate solidification. As the liquid cools, some of it solidifies so that the vapor, liquid, and solid phases all coexist (Triple Point). The solid phase (crystal) grows until it is contiguous throughout the entire capsule. When the ice crystal is fully contiguous the features in the ice can be observed and quantified.

During the layering process, the inner surface of the layering sphere is adjusted to be colder than the target, and heat is transferred from the target to the sphere by conduction, convection, and radiation. As a consequence, the farther the ice surface is from the wall of the layering sphere the warmer it will be. The principle of layering is that the vapor pressure above a warmer portion of the ice will be greater than the vapor pressure above a cooler portion of the ice. Since this is thermodynamically unstable, the thicker ice will sublime (go directly from the solid to the vapor phase), the vapor will then diffuse across the capsule interior, and condense where the ice is cooler and, hence thinner.

Eventually the inner ice surface will closely approximate an isotherm. Although the inner ice surface is almost "isothermal," that does not mean that the ice is uniformly thick. If the thermal resistance between the ice and the plastic capsule wall varies around the target, the ice thickness will vary so as to maintain an isothermal inner surface. Similarly, if the plastic wall varies in thickness or the thermal conductivity of the ice varies (because of crystallographic variations), the ice thickness may vary, even though the inner surface is on an isotherm.

The critical steps for attaining a uniformly thick ice layer are to control the heat flux into the ice, the heat flux out of the ice, and the final temperature of the ice. The uniformity of the heat flux into the ice is controlled by the stability of the OPO laser. The uniformity of the heat flux out of the target is controlled by (1) how well the target is positioned in the center of the layering sphere and (2) the temperature uniformity of the layering sphere. The density of the helium "exchange gas" in the layering sphere is also important. At pressures below 0.01 Torr, below the continuum region, the thermal conductivity and time constant of the gas depends on the pressure.

The most critical factor in forming good-quality ice layers is to allow the ice to solidify gradually over at least 5 min, avoiding instant freezing and to ensure that the final temperature of the ice is close to the triple point. To accomplish this it is necessary to first accurately establish the temperature on the layering sphere where the target freezes. To do so, a target must be cooled below the triple point to freeze (this freezing may be rapid), and then a rough layer must be allowed to form. The target is then warmed in 10-mK steps until it melts. It is imperative to wait at each layering-sphere temperature until the target has reached equilibrium. The temperature step at which the solid phase disappears is an accurate estimate of the layering-sphere temperature that corresponds to the triple point of the fuel in the capsule.

Since freezing a liquid to form a solid is ultimately a stochastic process where random cryostallographic defects formed during solidification can have variable effects on the thermal conductivity of the ice, there will be a variation in ice roughness even when identical layering procedures are followed. It may also be necessary to melt a poor-quality ice layer and to repeat the solidification process. If the layer is repeatably rough, and the operator has confidence in the accuracy of the parameter determinations (stable OPO power, adequate exchange gas pressure, and accurate "triple point determination"), it is likely that target variables (particularly variable capsule wall thickness) or layering

sphere aberrations (ablation damage to the layering sphere affecting the uniformity of the illumination, fiber optic alignment, or damage issues) dominate the layering process for the particular target and/or sphere.

8.3.2 Determination of Triple Point (via TPA)

The triple point of a material is the combination of temperature and pressure at which the vapor, liquid, and solid phases are all in equilibrium. This is the point on a phase diagram where the solid–vapor, solid–liquid, and liquid–vapor equilibrium lines all meet. The layering process requires the target to be held at triple point conditions.

Determining the layering-sphere temperature setting required for a given target to achieve triple point is a time-consuming process. The intent of the Triple Point Automation (TPA) module is to automate the data acquisition process. An operator activates this module after entering the operating parameters. TPA changes the Lakeshore temperature in steps and allow it to soak a determined amount of time at the new temperature before acquiring an image and the associated process data. When the cycle has been completed, these images are reviewed to determine the triple point temperature. Figure 8.3-1 illustrates the temperature ramp that results from the temperature step changes and soak time.

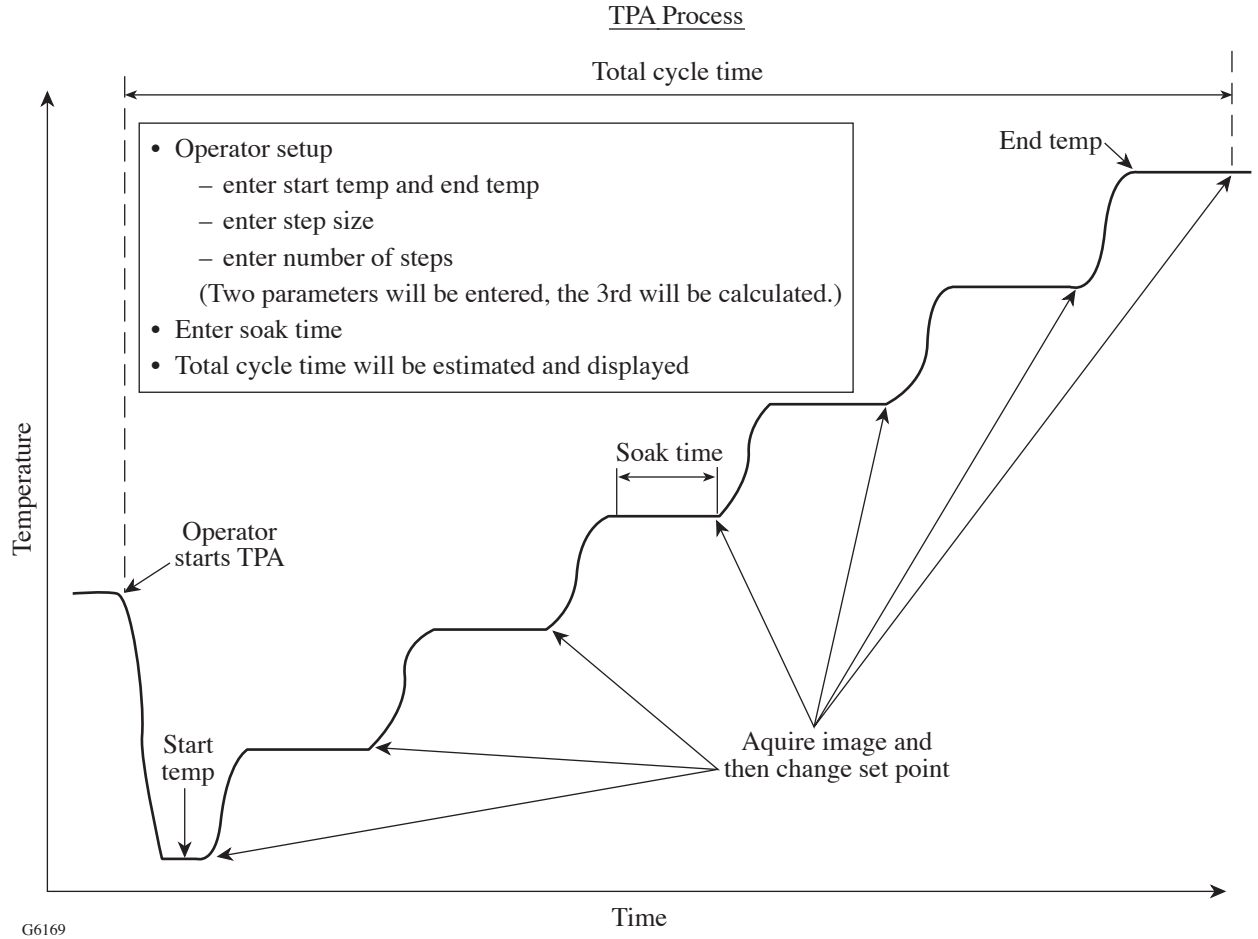

Figure 8.3-1
TPA temperature ramp and acquisition.

8.3.3 Layering Crystal Formation

Slow solidification of ice (up to 24 h) yields the best layer. The initial target condition is shown (puddle or melted target) in Fig. 8.3-2. The crystal growth can be seen in Fig. 8.3-3. A layered target with a low rms is shown in Fig. 8.3-4. It is critical to form the layer within 20 mK of the triple point to obtain a smooth layer (<5 μm). Establishing proper initial conditions is critical to the ultimate ice smoothness. Rapid cooling produces multifaceted morphology.

Extended layering durations (up to 2 days) do not always improve the smoothness. Rough layers (rms > 20) often remain rough. The roughness in all modes (up to ℓ = 30) increases when the temperature is reduced 1.8 K below triple point. The initial smoothness can be recovered by bringing the temperature just below triple point (within 5 mK). Poorly layered targets are shown in Fig. 8.3-5.

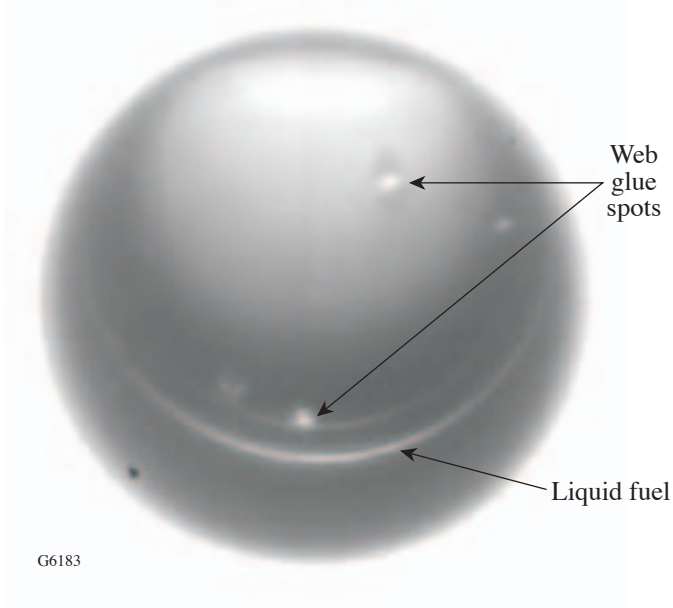

Figure 8.3-2
Initial target condition with liquid "puddle" at the bottom of the target.

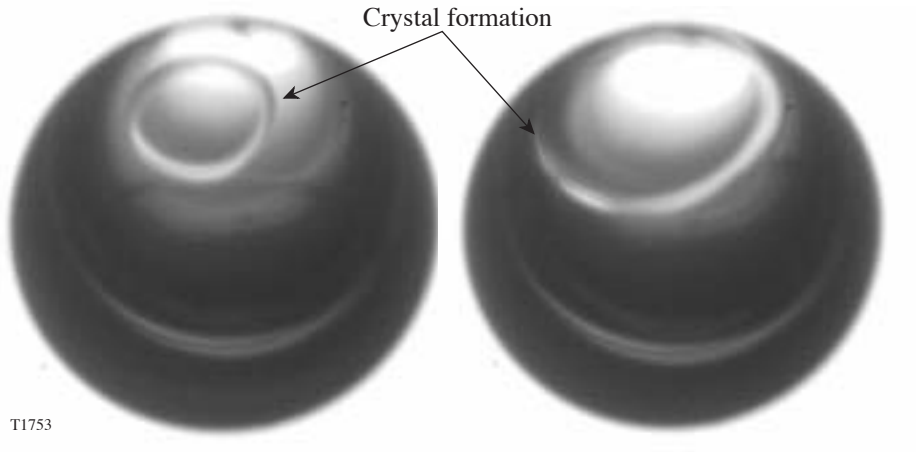

Figure 8.3-3
Crystal growth during the layering process.

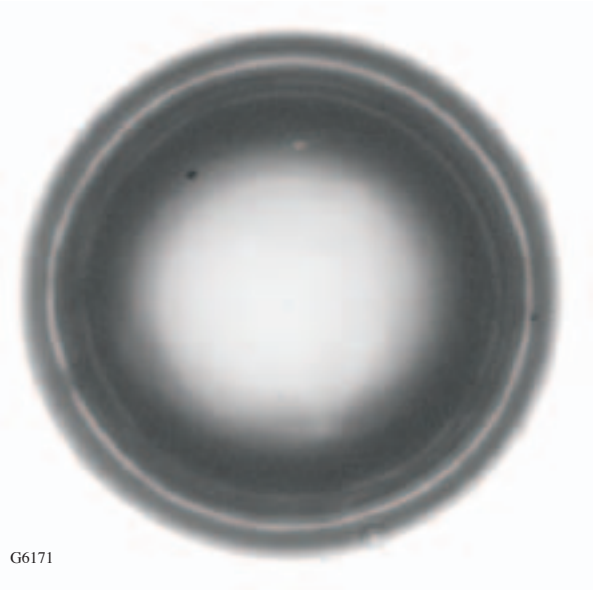

Figure 8.3-4
A layered target.

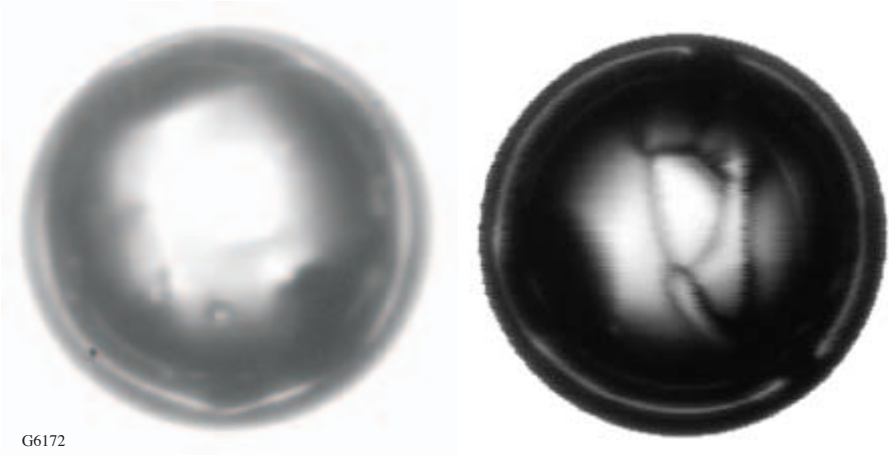

Figure 8.3-5
Images of poorly layered targets.

8.4 CHARACTERIZATION OF LAYERED TARGETS

The measurement system performance necessary to adequately characterize spherical cryo targets are very stringent. The following requirements must be met:

- Quantify the ℓ-mode composition of the surface for $1 < \ell < 50$; this corresponds to a 15-μm lateral resolution (at least an *f*/5 optical system).

- Adequate image quality must be achieved while looking through multiple shroud windows.

The target is illuminated from behind by a fiber-coupled LED at ~613 to 620 nm. A bright band in the transmitted image is due to internal reflection from the ice/gas interface (Fig. 8.4-1). The image is unique to the region of the ice along a great circle perpendicular to the viewing axis.

The two Dalsa 1M30P 12-bit, 1024 × 1024 scientific cameras are positioned nearly orthogonal to each other and are at slightly different elevations. These viewing axes correspond to the axes of the Target Viewing System in the Target Chamber. The X camera is pointed along an axis 12.7° above the horizontal, and the Y camera is pointed 26.6° above the horizontal. Because these views are angled relative to the targets axis of rotation, there is a region at the target's poles that cannot be seen regardless of the target orientation.

Each individual view of the target allows only the thickness of the ice ring that is perpendicular to the viewing axis to be quantified. Rotating the target and acquiring multiple images achieves a more-complete measure of the ice roughness. Currently the target is rotated through increments of 15°, and 7 images are acquired in quick succession at each position. A typical target rotation will contain 175 images (7 images at 25 different rotational settings).

Once the rotation set has been taken, the images are analyzed using Matlab routine. This software finds the perimeter of the plastic and the center of the target and determines the distance of the ice's inner surface from the center of the target. These data are used to measure the roughness of the ice, which is reported as the coefficients of a cosine Fourier transform. A summary sheet generated for each image includes the original image, the target parameters, the unwrapped image, inner (ice layer) and outer (shell) edge profiles, rms roughness, and power spectrum. This summary is stored in PDF format for later use.

The quality of the shadowgraphs is very high, showing a multitude of rings that are produced by various rays through the target (Fig. 8.4-1). The "standard" intense ring pattern follows a ray path (*b*) with one total internal reflection from the inner surface. The same spot on the inner surface is also probed by the rays on path (*u*). In fact, a number of rays suffer several internal bounces similar to the

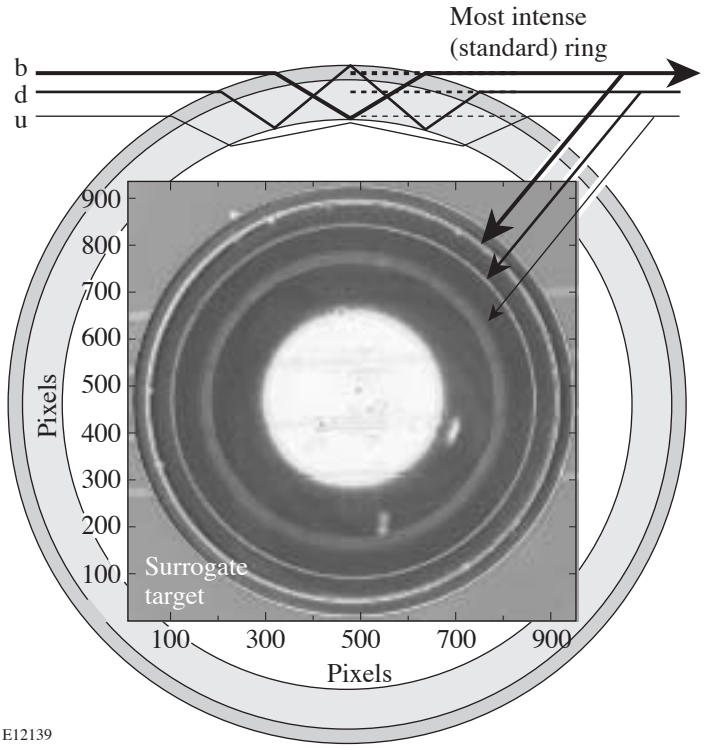

Figure 8.4-1
Shadowgraph of a thick CH surrogate target revealing a number of bright rings. The ray diagram shows the ray paths that give rise to the main rings visible in the experimental image. These rings and their associated ray paths have been uniquely identified using numerical simulations.

"*u*" rays; they all probe the inner surface from the inside and produce very sharp, closely spaced rings with a short focal depth. In addition, "*d*" rays form an intermediate, fairly strong ring and probe the apex of the outer surface.

All of these rings have been uniquely identified using spherically symmetric numerical simulations. Most of the information regarding ice-layer thickness and its variations is obtained from the strongest ring formed by the "*b*" rays. The weaker inner rings, however, can yield important additional information relating to the ice–plastic shell interface, a process LLE is studying in real, layered cryogenic targets.

Automated three-dimensional (3-D) characterization is provided by using TRIAS to rotate the target, center the target, and acquire images. The series of images is then analyzed by the 3-D analysis package Matlab, an application that provides 3-D images of the target as well as analysis of the layer quality along multiple axes. Accurate 3-D reconstructions and detection of isolated features require many segment images. The 3-D analysis smoothes the data from each segment image and then maps the data onto a sphere as shown above. The information for the low-order modes is then calculated.

A typical shadowgram of a cryogenic target is shown in Fig. 8.4-2. The outermost bright ring inside the target surface is representative of the ice layer. The breaks in the ring are caused by either outer-surface imperfections or ice nonuniformities. These data are unfolded to form a rectangular image in radius (~100-μm band) and angle (360°). Breaks in the ring or surface problems (e.g., tangent spider silks) are appropriately interpolated. As many as 30 shadowgrams are taken at different angles, and average power spectra of the ice-surface variations are generated using FFT's. An average power spectrum is shown in Fig. 8.4-3.

A 3-D image of the ice-layer thickness shown in Fig. 8.4-4. The ice-thickness variations are shown in color (see color bar). The ice thickness can be calculated from the location of the bright ring in the shadowgram as well as from the D_2-fill pressure. The two independent measurements agree to within 3%, which is considered to be in excellent agreement.

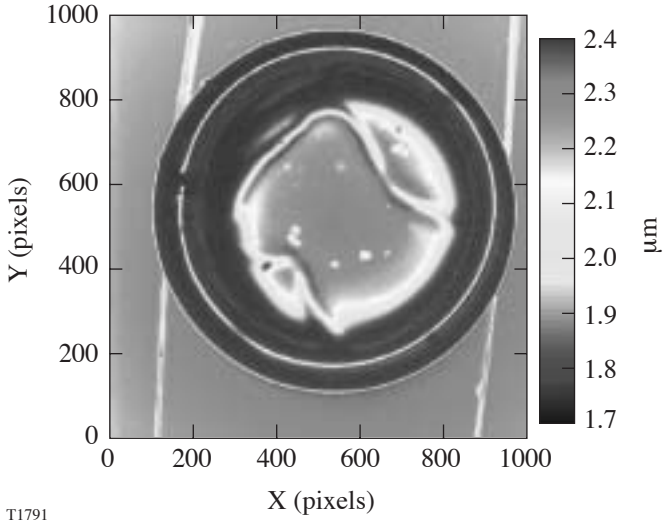

Figure 8.4-2
Shadowgram of a cryogenic target with an ~100-μm ice layer.

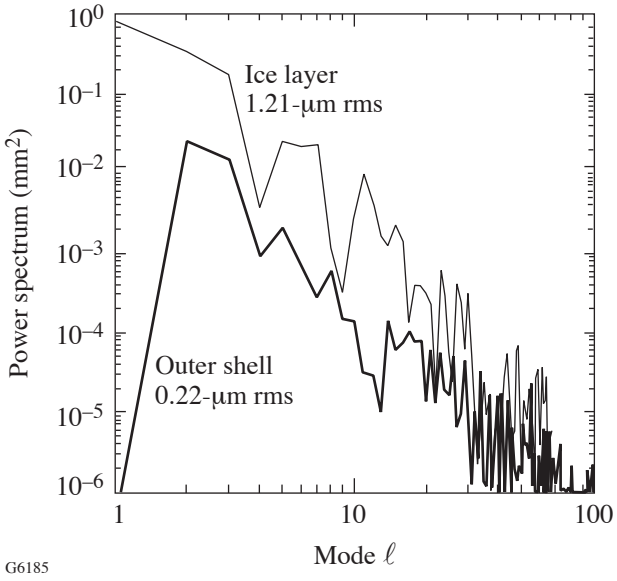

Figure 8.4-3
Average power spectra of outer target surface and ring due to the ice layer.

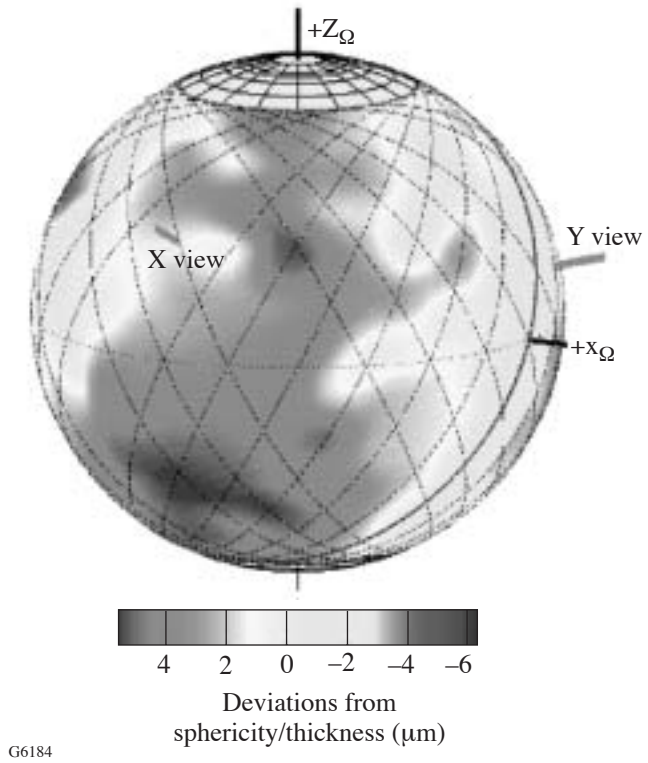

Figure 8.4-4
Three-dimensional view of ice-layer-thickness variations obtained from a large number of shadowgrams.

The shadowgraphic technique has been analyzed using a 1-D ray-trace simulation and a 3-D optics code (courtesy of Prof. Thomas Brown, The Institute of Optics). The former gave precise information about the locations and origins of the many different rings that may be observed. By contrast, the optics code was used to understand the importance of outer-surface perturbations on perceived inner-ice-surface perturbations. Figure 8.4-5 shows simulated bright-ring positions for a target with a perfect outer surface and a perturbed inner ice layer. The ice-layer perturbations are fully measurable in this case (a). For a perturbed outer surface and a perfect ice layer, the ring may or may not be distorted depending on the exact location of the outer-surface perturbations [(b) and (c)]. This demonstrates that outer-surface perturbations must be kept small compared to the expected inner-ice-surface perturbations. It also confirms observations where small outer-surface perturbations or miniscule dust particles may lead to partial or complete disruptions of the ring.

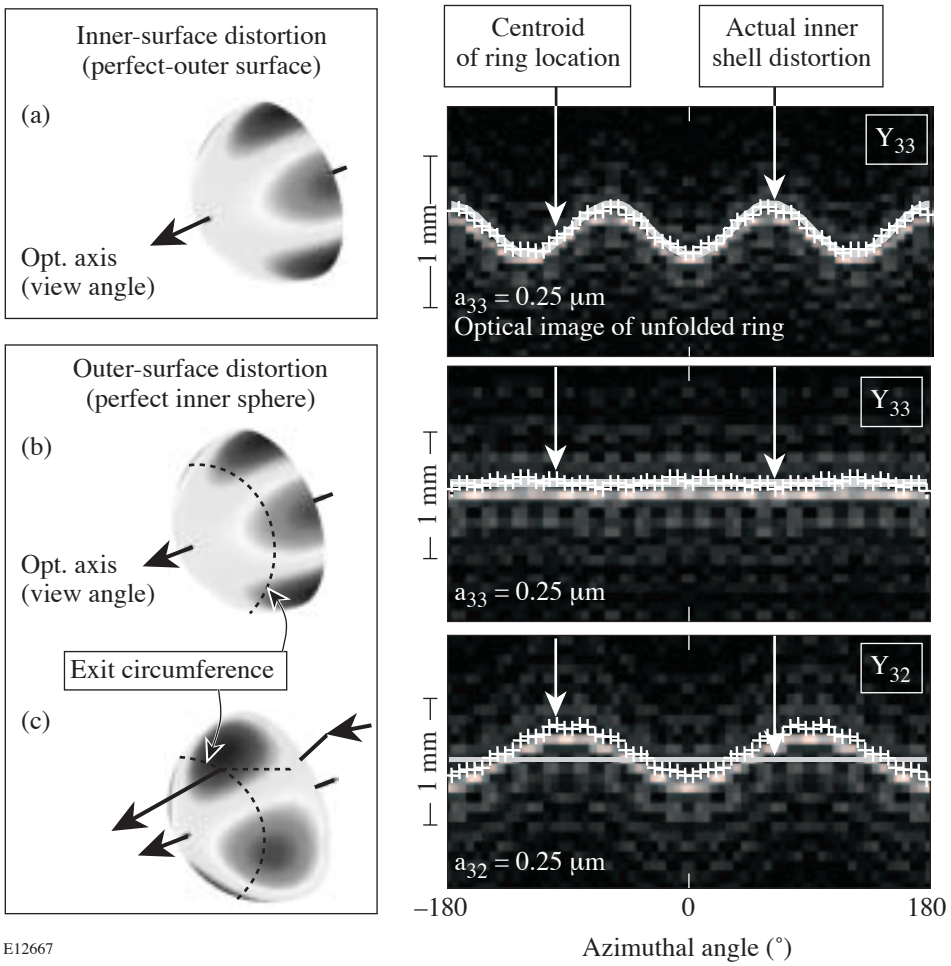

Figure 8.4-5
Results obtained with a 3-D optics imaging code for a perfect outer target surface with inner-ice-layer perturbations (Y_{33} with 0.25-μm amplitude). (a) The inner-ice-surface perturbations are easily measurable. Outer surface perturbations may cause apparent ice-surface perturbations as shown in (b) and (c), depending on their locations.